MOLECULAR AND CELLULAR BIOLOGY, July 1996, p. 3781–3788 Vol. 16, No. 7
0270-7306/96/$04.00+0

Nitric Oxide and Oxidative Stress (H_2O_2) Control Mammalian Iron Metabolism by Different Pathways

KOSTAS PANTOPOULOS, GÜNTER WEISS,† AND MATTHIAS W. HENTZE*

Gene Expression Programme, European Molecular Biology Laboratory, Heidelberg, Germany

Received 14 February 1996/Returned for modification 2 April 1996/Accepted 9 April 1996

Several cellular mRNAs are regulated posttranscriptionally by iron-responsive elements (IREs) and the cytosolic IRE-binding proteins IRP-1 and IRP-2. Three different signals are known to elicit IRP-1 activity and thus regulate IRE-containing mRNAs: iron deficiency, nitric oxide (NO), and the reactive oxygen intermediate hydrogen peroxide (H_2O_2). In this report, we characterize the pathways for IRP-1 regulation by NO and H_2O_2 and examine their effects on IRP-2. We show that the responses of IRP-1 and IRP-2 to NO remarkably resemble those elicited by iron deficiency: IRP-1 induction by NO and by iron deficiency is slow and posttranslational, while IRP-2 induction by these inductive signals is slow and requires de novo protein synthesis. In contrast, H_2O_2 induces a rapid posttranslational activation which is limited to IRP-1. Removal of the inductive signal H_2O_2 after ≤15 min of treatment (induction phase) permits a complete IRP-1 activation within 60 min (execution phase) which is sustained for several hours. This contrasts with the IRP-1 activation pathway by NO and iron depletion, in which NO-releasing drugs or iron chelators need to be present during the entire activation phase. Finally, we demonstrate that biologically synthesized NO regulates the expression of IRE-containing mRNAs in target cells by passive diffusion and that oxidative stress endogenously generated by pharmacological modulation of the mitochondrial respiratory chain activates IRP-1, underscoring the physiological significance of NO and reactive oxygen intermediates as regulators of cellular iron metabolism. We discuss models to explain the activation pathways of IRP-1 and IRP-2. In particular, we suggest the possibility that NO affects iron availability rather than the iron-sulfur cluster of IRP-1.

The iron-regulatory proteins IRP-1 and IRP-2 are cytoplasmic mRNA-binding polypeptides which regulate several mRNAs containing iron-responsive elements (IREs) in their untranslated regions (reviewed in references 30, 31, and 38). IRP binding to the IREs in the 5′ untranslated regions of ferritin and erythroid 5-aminolevulinate synthase mRNAs represses their translation (12, 37, 47), whereas binding of IRPs to multiple IREs in the 3′ untranslated region of transferrin receptor (TfR) mRNA confers stability against targeted endonucleolytic degradation (2, 4, 39). Therefore, the signals that control IRE binding by IRPs regulate the expression of these IRE-containing mRNAs and exert a profound influence on cellular iron metabolism.

IRP-1, formerly referred to as IRE-BP, FRP, IRF, or IRP, has two mutually exclusive activities, which are switched by changes in an iron-sulfur cluster (6). With a fully assembled 4Fe-4S cluster in iron-replete cells, IRP-1 is a cytoplasmic aconitase, whereas in its apoprotein form in iron-deficient cells, IRP-1 binds with high affinity to IREs (10, 14, 19, 20, 28). Posttranslational interconversion between the 4Fe-4S- and apoprotein forms thus constitutes the basis for the regulation of IRP-1 activities by iron (22, 41, 46). In addition to iron, nitric oxide (NO) acts as an independent regulatory signal (8, 42, 49). Very recently, H_2O_2 was revealed to regulate IRP-1 (36, 43). The activation of IRP-1 by H_2O_2 represents a direct regulatory link between cellular iron metabolism and oxidative stress, an intriguing constellation in light of Fenton chemistry, e.g., the generation of highly toxic hydroxyl radicals by ferrous iron and H_2O_2. On the basis of biochemical evidence, iron deficiency, NO, and H_2O_2 all appear to induce the conversion of 4Fe-4S IRP-1 to apoIRP-1 (19, 42, 43), although this interpretation will require further investigation by more-direct analytical methods.

IRP-2, formerly also known as IRE-BP2, IRF_B, or IRP_B, is less well characterized. IRP-2 activity was originally identified in murine cells (18, 23) and appears to be present in almost all species and cell types expressing IRP-1 (16, 22, 23, 45). Rat IRP-2 exhibits 61% amino acid identity and 79% similarity with rat IRP-1 (16). The two proteins differ most significantly in their amino termini: IRP-2 contains a 73-amino-acid insertion encoded by a unique exon (16, 27). In contrast to IRP-1, IRP-2 lacks aconitase activity (18), despite the conservation of 16 of the 18 aconitase active-site residues. The three cysteine residues that coordinate the Fe-S cluster in IRP-1 are conserved in IRP-2 (16). However, IRP-2 regulation does not appear to require the formation of an IRP-1-like cubane iron-sulfur cluster (27). IRP-2 is degraded in iron-replete cells and accumulates in iron-deficient cells requiring de novo protein synthesis (18, 22, 41, 45). The 73-amino-acid insertion contains a cysteine-rich element which mediates iron-dependent degradation of IRP-2, possibly by the proteasome pathway (17, 27).

We have previously shown that like IRP-1, activity IRP-2 activity is increased by NO (42, 49). However, no data regarding the effect of H_2O_2 on IRP-2 are available. As both NO and H_2O_2 are frequently considered to be members of a family of diffusible reactive signalling molecules (for a review, see reference 29), we characterized and delineated the pathways of the responses of IRP-1 and IRP-2 to these two signals and compared them with the responses elicited by iron starvation.

MATERIALS AND METHODS

Cell treatments and reagents. Murine B6 and Ltk⁻ fibroblasts were grown in Dulbecco modified Eagle medium (DMEM) supplemented with 2 mM glu-

* Corresponding author. Mailing address: Gene Expression Programme, European Molecular Biology Laboratory, Meyerhofstrasse 1, D-69117 Heidelberg, Germany. Phone: 49-6221-387 501. Fax: 49-6221-387 518. Electronic mail address: hentze@embl-heidelberg.de.

† Present address: Department of Internal Medicine, University Hospital, A-6020 Innsbruck, Austria.

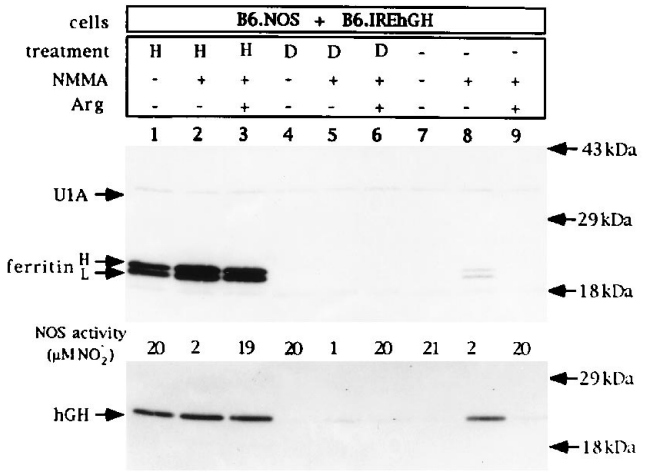

FIG. 1. Intercellular signalling to IRPs by NO. B6.IREhGH cells were cocultured with B6.NOS cells and treated with 100 μM heme arginate (H) (lanes 1 to 3) or 100 μM desferrioxamine (D) (lanes 4 to 6) or left as controls (lanes 7 to 9). NOS activity either was not modulated (lanes 1, 4, and 7), was inhibited by treatment with 400 μM NMMA (lanes 2, 5, and 8), or was inhibited and restored by simultaneous treatment with 400 μM NMMA and 10 mM L-arginine (lanes 3, 6, and 9). The assay of nitrite from the culture supernatant reflects NOS activity. SDS-PAGE of a quantitative immunoprecipitation with hGH, ferritin, and U1A (internal control) antibodies is shown. Immunoprecipitated hGH derived from B6.IREhGH cells (bottom panel) and ferritin (heavy [H] and light [L] chains) and U1A derived from both B6.NOS and B6.IREhGH cells (top panel) are indicated by arrows on the left. The positions of molecular mass standards are shown by arrows on the right.

tamine, 100 U of penicillin per ml, 0.1 ng of streptomycin per ml, and 10% fetal calf serum. Treatments with H_2O_2 were performed as described previously (43). Desferrioxamine, DL-penicillamine, paraquat, N^G-monomethyl-L-arginine (NMMA), cycloheximide, and antimycin A were purchased from Sigma (St. Louis, Mo.). Sodium nitroprusside (SNP), 3-morpholinosydnonimine (SIN-1), 1-hydroxy-2-oxo-3,3-bis-(3-aminoethyl)-1-triazene (NOC-18), and *S*-nitroso-*N*-acetyl-DL-penicillamine (SNAP) were from Alexis Corporation (Läufelfingen, Switzerland). Nitroglycerine and heme arginate were generous gifts of Schwarz Pharma AG (Monheim, Germany) and Leiras Oy (Turku, Finland), respectively. Treatment conditions are described in detail in Results and in the figure legends.

Coculture of B6.NOS and B6.IREhGH fibroblasts. The B6.NOS and B6.IREhGH cell lines are derived from the murine fibroblast cell line B6 by stable transfection and were maintained in Dulbecco modified Eagle medium supplemented with additives and 0.1 mM sodium hypoxanthine–0.4 μM aminopterin–16 μM thymidine. B6.NOS cells express the murine macrophage nitric oxide synthase (NOS) (42), and B6.IREhGH cells (referred to as FerGH in reference 7) express an IRE-containing human growth hormone (hGH) mRNA. B6.NOS cells (3×10^6) and B6.IREhGH cells (1×10^6) were cocultured. Following incubation with 5 mM sodium butyrate (to augment transcription from the transfected genes) plus 5 μM ferric ammonium citrate (to prevent cellular iron deprivation) for 8 h, the cells were treated overnight in fresh medium with or without 400 μM NMMA (a substrate analog inhibitor of NOS) or 10 mM L-arginine (substrate of NOS). Nitrite production in the supernatant of the culture was assessed by the Griess color reaction (15), and 100 μM heme arginate or 100 μM desferrioxamine was added. After 4 h, cells were labelled for 2 h with [^{35}S]methionine (50 μCi/ml). Heme arginate, desferrioxamine, NMMA, or L-arginine treatment was continued during metabolic labelling.

Immunoprecipitation of ^{35}S-labelled proteins. Quantitative immunoprecipitation from equal amounts of trichloroacetic acid-insoluble radioactivity was performed as described previously (37). Following normalization, half of the lysate was subjected to immunoprecipitation with polyclonal hGH antibodies (National Hormone and Pituitary Program, Baltimore, Md.). The other half was incubated with ferritin antibodies (Boehringer Mannheim, Indianapolis, Ind.) and U1A antiserum (kindly provided by Iain Mattaj, EMBL). Immunoprecipitated ^{35}S-labelled polypeptides were analyzed by sodium dodecyl sulfate-polyacrylamide gel electrophoresis (SDS-PAGE) and visualized by fluorography and autoradiography.

EMSA. Electrophoretic mobility shift assays (EMSAs) were performed as described earlier (34) with a radiolabelled IRE probe (42).

RESULTS

Intercellular signalling to IRPs by nitric oxide. In cells expressing NOS, NO activates endogenous IRP-1 and IRP-2 (8, 42, 49). Since much of the physiology of NO-mediated responses is based on intercellular signalling by NO diffusion from NOS-expressing cells to target cells, the effect of intercellular NO signalling to IRPs was directly investigated. We utilized B6 fibroblasts that were stably transfected with a murine macrophage NOS plasmid (B6.NOS cells) (42) and B6.IREhGH cells, which express an IRE-containing hGH reporter mRNA. These two otherwise identical cell lines were cocultured at a ratio of 3 (B6.NOS) to 1 (B6.IREhGH). Following metabolic labelling with [^{35}S]methionine, translation of the hGH reporter mRNA was analyzed by hGH immunoprecipitation (Fig. 1, bottom panel). As a result of iron-dependent changes in IRP activities, hGH biosynthesis is elevated in cells treated with heme arginate (Fig. 1, bottom panel, lanes 1 to 3) and is inhibited in cells treated with the iron chelator desferrioxamine (lanes 4 to 6). NO release by B6.NOS cells results in complete repression of hGH biosynthesis in B6.IREhGH cells (Fig. 1, lane 7), which is restored by blocking NO synthesis with the stereospecific inhibitor NMMA (lane 8). Simultaneous treatment with 400 μM NMMA and an excess of substrate (10 mM L-arginine) restores NO release (evident from the nitrite levels in the culture supernatant) and the inhibition of hGH biosynthesis (Fig. 1, lane 9). In cells pretreated with heme, hGH expression is also regulated by NO, albeit less extensively (compare lanes 1 and 3 with lane 2). As controls, ferritin and the non-IRP-regulated spliceosomal protein U1A were immunoprecipitated (Fig. 1, top panel). While U1A levels remain unchanged, ferritin biosynthesis (positive control) in B6.NOS (75%) and B6.IREhGH (25%) cells is regulated by iron and NO, paralleling the expression of hGH in B6.IREhGH cells. We conclude that NO regulates iron metabolism by both intercellular and intracellular signalling to IRPs.

To reproduce intercellular NO signalling to study the NO-mediated activation pathway in a pharmacologically defined way, different NO donors were tested for their effects on IRPs. B6 cells were treated for 4 and 8 h with the following compounds at 100 μM: the NO donors nitroglycerine, NOC-18, and SNAP, the SNAP precursor DL-penicillamine, SNP (an agent used to nitrosylate thiol groups via NO^+ [35]), SIN-1 (which simultaneously releases NO and superoxide anion, yielding peroxynitrite [11]), the superoxide anion-releasing substance paraquat, and a combination of SNAP and paraquat. Cytoplasmic extracts were analyzed for IRE-binding activity by EMSA with a radiolabelled IRE probe.

Treatment with 100 μM NOC-18 and SNAP for 4 and 8 h activates IRP-1 (Fig. 2, top panel, lanes 5 to 6 and 13 to 14), in contrast to treatment with the SNAP precursor DL-penicillamine (lanes 7 and 15), indicating that the effect of SNAP results from the release of NO. Treatment with nitroglycerine, SNP, and SIN-1 fails to activate IRP-1 under these experimental conditions. Consistent with our previous observations, paraquat partially induces IRP-1 activity (Fig. 2, lanes 9 and 17), possibly by dismutation of superoxide anion to H_2O_2 (43). Activation of IRP-1 by SNAP is not augmented under conditions which favor generation of peroxynitrite (lanes 8 and 16), in agreement with recent observations (44). Treatment of cell extracts with 2% 2-mercaptoethanol (2-ME) to activate 4Fe-4S IRP-1 in vitro (24) confirmed the equal loading of all lanes (Fig. 2, bottom panel). Interestingly, faint IRE–IRP-2 complexes appear following 8 h of treatment with NOC-18 and SNAP (Fig. 2, lanes 13, 14, and 16), but the low level of IRP-2 expression in B6 cells impeded further interpretation. Higher

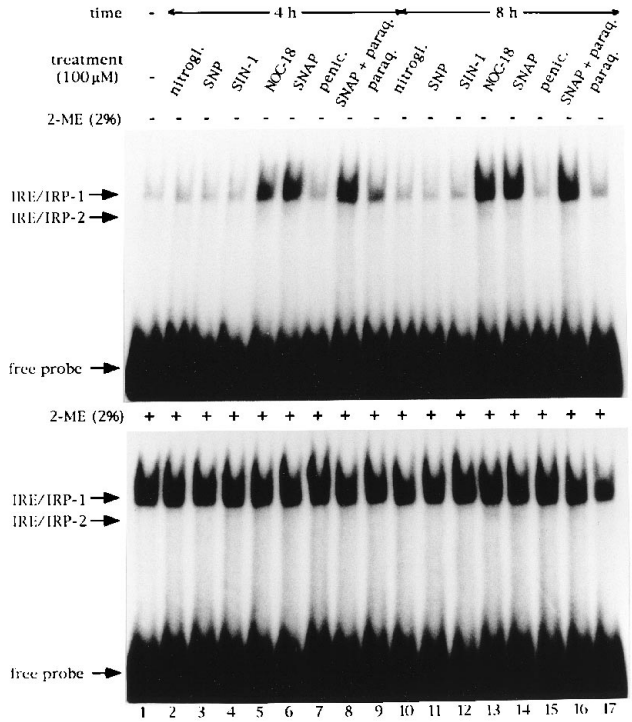

FIG. 2. Pharmacological modulation of the IRE-binding activities of IRP-1 and IRP-2. B6 fibroblasts were left untreated (lane 1) or were treated for 4 h (lanes 2 to 9) or 8 h (lanes 10 to 17) with the following compounds at 100 μM: nitroglycerine (nitrogl.) (lanes 2 and 10), SNP (lanes 3 and 11), SIN-1 (lanes 4 and 12), NOC-18 (lanes 5 and 13), SNAP (lanes 6 and 14), DL-penicillamine (penic.) (lanes 7 and 14), SNAP plus paraquat (paraq.) (lanes 8 and 15), or paraquat (lanes 9 and 17). SNAP was dissolved in 75% dimethyl sulfoxide; all other solutions were aqueous. Cytoplasmic extracts (10 μg) were analyzed by EMSA with 25,000 cpm of ^{32}P-labelled IRE probe in the absence (top panel) or presence (bottom panel) of 2% 2-ME. The positions of IRE–IRP-1 and IRE–IRP-2 complexes and of excess free IRE probe are indicated by arrows. The solvent dimethyl sulfoxide alone has no effect on IRE-binding activities (not shown).

concentrations of SNAP (up to 1 mM) were found not to augment IRP activation (data not shown). Since SNAP appears to be a suitable NO donor with well studied pharmacological properties (NO release in aqueous solutions is linear over a wide concentration range, and 100 μM SNAP yields ~1.4 μM NO per min at 37°C [11]), 100 μM SNAP was used in all subsequent experiments.

Two kinetic classes of IRP activation by H_2O_2, NO, and iron deficiency. Three different signals have been found to activate IRP-1: H_2O_2, NO, and iron deficiency. To compare the activation kinetics of IRP-1 in response to these signals and to investigate the responsiveness of IRP-2 to H_2O_2 and NO, we examined murine Ltk$^-$ cells, a fibroblastic cell line that expresses higher IRP-2 levels than B6 fibroblasts. The cells were treated with 100 μM H_2O_2, SNAP, or desferrioxamine for 30 min to 12 h, and IRE-binding activities were assessed by EMSA (Fig. 3). As recently shown for IRP-1 (36, 43), activation by H_2O_2 is rapid: after 30 min, IRP-1 activity is strongly induced, and it remains elevated for 8 h of treatment (Fig. 3, lanes 1 to 7). We noticed that cell viability was affected by prolonged H_2O_2 treatment (>4 h). Importantly, H_2O_2 does not significantly activate IRP-2 over 8 h of treatment (Fig. 3, lanes 1 to 7), which is in contrast to the rapid activation of IRP-1. Similarly, treatment with less toxic concentrations of H_2O_2 (10, 25, and 50 μM H_2O_2 for 4, 6, and 8 h) also failed to activate IRP-2. Under these conditions, IRP-1 was activated by 50 μM H_2O_2 (data not shown). In some experiments, ≤ 5% of the IRP-2 activity elicited by iron starvation or NO treatment was induced by H_2O_2 (compare lanes 1 to 7 with lane 13 in Fig. 3). Since this contributes very marginally to the total H_2O_2-mediated increase of IRE-binding activity (lanes 1 to 7), H_2O_2 emerges as an IRP-1-specific signal.

In contrast to the case for H_2O_2, we found that the activation of IRP-1 and IRP-2 upon treatment with SNAP is surprisingly slow, with a kinetic induction pattern closely resembling that of iron deficiency (Fig. 3, compare lanes 8 to 13 with lanes 14 to 19). Both IRP-1 and IRP-2 respond slowly to NO, and maximal activation requires, even with higher concentrations (data not shown), administration of SNAP for 8 to 12 h (Fig. 3, lanes 1 and 14 to 19). A similar procedure with the SNAP precursor DL-penicillamine does not activate IRP-1 or IRP-2 (data not shown). Hence, the activation of IRPs can be divided into two kinetic classes: a fast response to H_2O_2, which is restricted to IRP-1, and a delayed response to iron deficiency or NO, which activates both IRP-1 and IRP-2.

The delayed-response mechanism of IRP-1 and IRP-2. To uncover similarities and/or differences between the mechanisms of the delayed response to NO and to iron deficiency, we first treated Ltk$^-$ fibroblasts for 12 h with 100 μM desferrioxamine or SNAP in the presence or absence of the protein synthesis inhibitor cycloheximide (40 μM). Consistent with our previous findings (41), cycloheximide does not prevent activation of IRP-1, but it completely abolishes the appearance of IRP-2 activity in response to desferrioxamine (Fig. 4, lanes 1 to 4). Under the same conditions, cycloheximide does not prevent activation of IRP-1 by SNAP, while it completely inhibits IRP-2 (Fig. 4, lanes 5 and 6). Thus, NO activates IRP-1 and

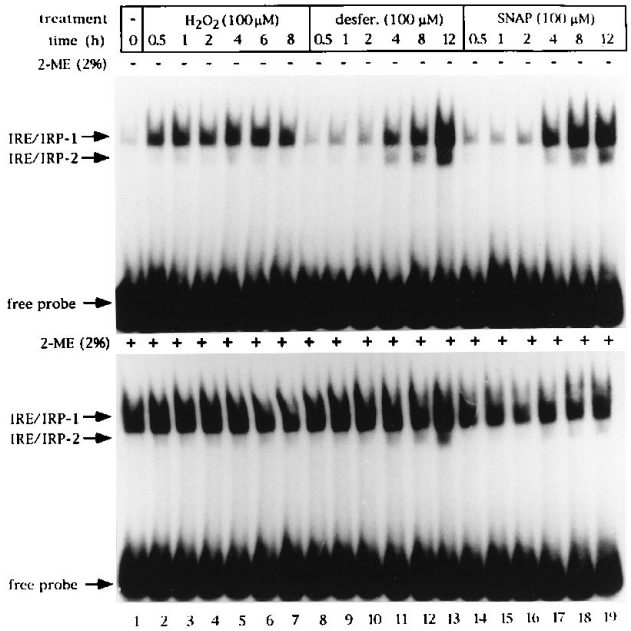

FIG. 3. Exclusive rapid activation of IRP-1 by H_2O_2. Ltk$^-$ fibroblasts were left untreated (lane 1) or were treated for 30 min, 1 h, 2 h, 4 h, 6 h, and 8 h (lanes 2 to 7, respectively) with 100 μM H_2O_2 or for 30 min, 1 h, 2 h, 4 h, 8 h, and 12 h with 100 μM desferrioxamine (desfer.) (lanes 8 to 13, respectively) or 100 μM SNAP (lanes 14 to 19, respectively). H_2O_2 and SNAP were replaced with fresh solutions after 4 and 6 h, respectively. Cytoplasmic extracts (25 μg) were analyzed by EMSA with 25,000 cpm of ^{32}P-labelled IRE-probe in the absence (top panel) or presence (bottom panel) of 2% 2-ME. The positions of IRE–IRP-1 and IRE–IRP-2 complexes and of excess free IRE probe are indicated by arrows.

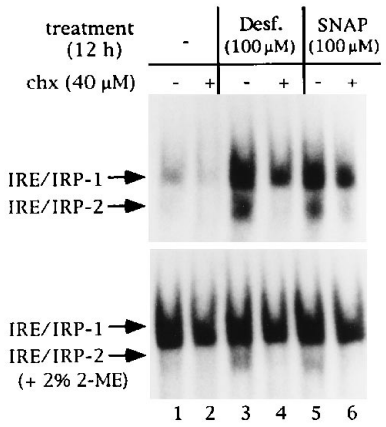

FIG. 4. Activation of IRP-1 by NO is posttranslational, while NO activation of IRP-2 requires de novo protein synthesis. Ltk$^-$ fibroblasts were left untreated (lanes 1 and 2) or were treated for 12 h with 100 μM desferrioxamine (Desf.) (lanes 3 and 4) or 100 μM SNAP (lanes 5 and 6) in the absence (lanes 1, 3, and 5) or presence (lanes 2, 4, and 6) of 40 μM cycloheximide (chx), which completely blocks protein synthesis under these conditions (41). SNAP was replaced with fresh solutions after 6 h. Cytoplasmic extracts (25 μg) were analyzed by EMSA with 25,000 cpm of ^{32}P-labelled IRE probe in the absence (top panel) or presence (bottom panel) of 2% 2-ME. Only the IRE–IRP-1 and IRE–IRP-2 complexes are depicted.

IRP-2 in a separable manner and, concordant with the kinetic data, in a mode reflecting that of iron starvation.

We also examined the effect of okadaic acid, an inhibitor of type I/IIa protein phosphatases, on the activation of IRP-1 and IRP-2 by NO. We recently reported that okadaic acid prevented the fast activation of IRP-1 by H_2O_2 in B6 cells but not the delayed activation by desferrioxamine (43), suggesting the involvement of protein phosphatases I/IIa in the H_2O_2-mediated IRP-1 induction pathway. In a subsequent series of experiments using okadaic acid as a marker for IRP-1 induction by H_2O_2, we observed differences in the ability of okadaic acid to affect the H_2O_2 induction pathway. The effect of okadaic acid appears to be sensitive to the cell type and to the commercial preparation of okadaic acid used (data not shown). Since stress-mediated signal transduction pathways are interconnected and protein phosphatases can exert stimulatory and inhibitory functions within these pathways (26, 48), their complexity argues against the use of okadaic acid as an unambiguous marker for the H_2O_2-mediated induction of IRP-1. With these caveats in mind, okadaic acid was found not to affect the activation of IRP-1 and IRP-2 by NO (data not shown) and desferrioxamine (43).

Distinct responses of the fast- and the delayed-activation mechanisms to signal withdrawal: H_2O_2 triggers an induction phase and an execution phase. The kinetic and pharmacological data suggest that an oxidative-stress-mediated (phosphorylation-dependent) pathway may be responsible for the activation of IRP-1 by H_2O_2. In contrast, separable pathways lead to activation of IRP-1 (and IRP-2) by iron starvation and NO. To further delineate the fast- and the delayed-response pathways, we investigated the effect of signal withdrawal from the cells. SNAP, H_2O_2, or desferrioxamine was removed after a suboptimal activation time, and the cells were chased in the absence of the signal.

Ltk$^-$ cells were treated with 100 μM H_2O_2 for 5, 10, or 15 min and either harvested or chased for up to 1 h. Similarly, they were treated with 100 μM desferrioxamine or SNAP for 1 h and either harvested or chased for another 3 or 7 h. As controls, cells were treated with H_2O_2 for 1 h or with desferrioxamine or SNAP for 4 and 8 h. Treatment with 100 μM desferrioxamine or SNAP for 1 h does not activate IRP-1 or IRP-2 (Fig. 5A, lanes 1, 9, and 14). Removal of the effector followed by a chase for 3 h (lanes 10 and 15) or 7 h (lanes 12 and 17) does not activate IRP-1 or IRP-2. For activation of IRP-1 and IRP-2, the continuous presence of desferrioxamine or SNAP for 4 or 8 h is required (Fig. 5A, lanes 11, 13, 16, and 18).

H_2O_2 partially activates IRP-1 within 5 to 15 min, while complete activation is accomplished after 1 h (Fig. 5A) (43). In contrast to the responses to desferrioxamine or SNAP removal, IRP-1 is progressively activated after the withdrawal of H_2O_2 (Fig. 5A, lanes 3, 5, and 7). A 45-min chase (execution phase) following a 15-min treatment with H_2O_2 (induction phase) allows for maximal activation of IRP-1, which is indistinguishable from that when the effector is continuously present (compare lanes 6 and 7 with lane 8 in Fig. 5A). IRP-2 also appears to be marginally activated in this experiment (lanes 8 and 9). Exposure of cells to H_2O_2 for as short a time as 5 min, followed by a 55-min chase, also partially induces IRP-1 (Fig. 5A, lanes 1 to 3).

To study for how long the activation of IRP-1 is maintained in the absence of the inductive signal, Ltk$^-$ cells were first treated with 100 μM desferrioxamine or SNAP for 12 h and then chased without the inducer for 2, 4, 6, and 8 h. Under these conditions, IRP-1 remains induced for 4 to 6 h after desferrioxamine or SNAP withdrawal (data not shown). We then treated Ltk$^-$ cells with 100 μM H_2O_2 for 15 min or 1 h and chased for up to 8 h following removal of H_2O_2 (Fig. 5B). Consistent with the data in Fig. 5A, a 15-min pulse with H_2O_2 partially induces IRP-1, and the induction is completed within 1 h (compare lanes 1, 2, 3, and 8 in Fig. 5B). IRP-1 induced by a 15-min pulse of H_2O_2 remains active for at least 4 h (lanes 3 to 7). When cells are fully induced by treatment with H_2O_2 for 1 h, the effect lasts ~2 h longer (Fig. 5B, lanes 9 to 13). Thus, a transient exposure of cells to micromolar concentrations of H_2O_2 suffices to cause lasting IRP-1 activation.

Induction of IRP-1 by pharmacological modulation of mitochondrial respiration. A physiological role of IRP-1 may be based on its ability to respond to altered levels of reactive oxygen intermediates. Since the mitochondrial respiratory chain represents one of the major sources of reactive oxygen intermediates in eukaryotic cells, we asked whether oxidative stress generated by the respiratory chain regulates IRP-1 activity. We treated cells with antimycin A, an inhibitor of complex III that increases the mitochondrial generation of reactive oxygen intermediates (3). Treatment of B6 and Ltk$^-$ fibroblasts with 100 μM antimycin A for 2 h markedly induces IRP-1 in both cell lines (Fig. 6), comparable to the induction elicited by 100 μM exogenous H_2O_2 supplied for 1 h and desferrioxamine treatment for 8 h (compare lanes 1 to 4 and lanes 5 to 8). Similar to the effect of exogenous H_2O_2, antimycin A fails to induce IRP-2 in both cell lines, while IRP-2 is appreciably induced by iron deficiency. We conclude that respiratory chain activity affects IRP-1.

DISCUSSION

In this report, we delineate the signal-response relationships of the two central mammalian iron-regulatory proteins, IRP-1 and IRP-2. We identify signalling requirements for activation of their IRE-binding properties, which subject the IRE-containing mRNAs to posttranscriptional regulation and thus exert a profound influence on iron metabolism. The information concerning the activation of both IRPs by the three different effectors is summarized in Fig. 7: IRP-1 responds to NO and to

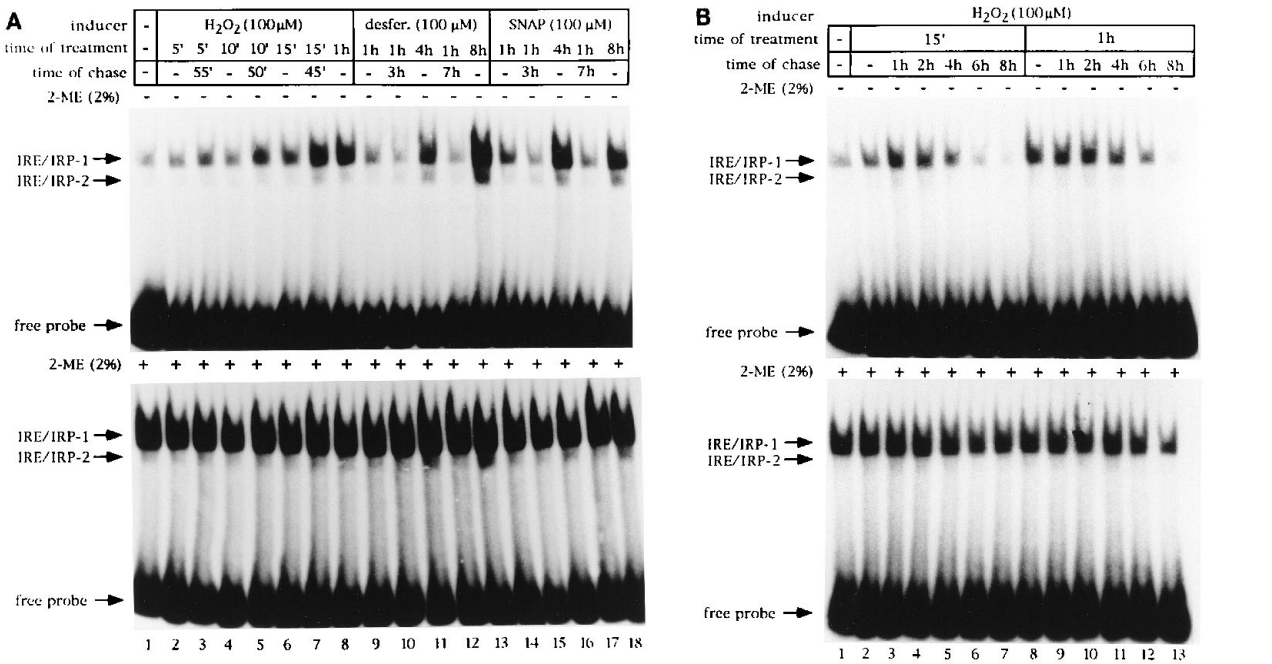

FIG. 5. Effects of signal withdrawal on IRP-1 and IRP-2 activation. (A) Ltk$^-$ fibroblasts were left untreated (lane 1) or were treated with 100 μM H_2O_2 for 5 min, 10 min, 15 min, and 1 h (lanes 2, 4, 6, and 8, respectively), 100 μM desferrioxamine (desfer.) for 1, 4, and 8 h (lanes 9, 11, and 13, respectively), or 100 μM SNAP for 1, 4, and 8 h (lanes 14, 16, and 18, respectively). Cells treated with H_2O_2 for 5, 10, or 15 min were washed and chased for 55, 50, or 45 min, respectively (lanes 3, 5, and 7); cells treated with desferrioxamine for 1 h were washed and chased for 3 or 7 h (lanes 10 and 12, respectively); and cells treated with SNAP for 1 h were similarly washed and chased for 3 or 7 h (lanes 15 and 17, respectively). (B) Ltk$^-$ fibroblasts were left untreated (lane 1) or were treated with 100 μM H_2O_2 for 15 min (lanes 2 to 7) or 1 h (lanes 8 to 13). Subsequently, cells were washed and chased for 0 h (lanes 2 and 8), 1 h (lanes 3 and 9), 2 h (lanes 4 and 10), 4 h (lanes 5 and 11), 6 h (lanes 6 and 12), or 8 h (lanes 7 and 13). Cytoplasmic extracts (25 μg) were analyzed by EMSA with 25,000 cpm of ^{32}P-labelled IRE probe in the absence (top panel) or presence (bottom panel) of 2% 2-ME. The positions of IRE–IRP-1 and IRE–IRP-2 complexes and of excess free IRE probe are indicated by arrows.

iron deficiency by delayed, okadaic acid-insensitive induction, while its activation by H_2O_2 is fast and, under certain conditions, sensitive to okadaic acid. In all cases the activation of IRP-1 is posttranslational and appears to result from the conversion of 4Fe-4S IRP-1 to apoIRP-1. On the other hand, IRP-2 responds only to iron deficiency and NO and is largely unaffected by H_2O_2. IRP-2 activation is slow, is insensitive to okadaic acid, and requires ongoing protein synthesis.

In regard to NO as a physiological regulator of iron metabolism, we show here that NO controls IRE-binding activity by intercellular signalling. We previously demonstrated that cytokine-induced J774.A1 and RAW 264.7 macrophage cells repress ferritin biosynthesis via endogenously produced NO (49) but, surprisingly, show decreased TfR mRNA levels (42). In contrast, target cells exposed to NO by intercellular signalling display the full spectrum of IRP-mediated responses, including translational repression of IREhGH mRNA and increased TfR mRNA expression (Fig. 1) (40). Thus, intercellular signalling by NO offers response diversity between the effector cells (induced macrophages) and target cells.

Kinetic separation into fast (H_2O_2) and delayed (NO) IRP-1 response pathways: mechanistic considerations. Our results show that the responses of IRPs to H_2O_2 and NO can be classified into two distinct kinetic classes: (i) fast responses to H_2O_2, involving rapid activation of IRP-1, and (ii) delayed responses to NO, involving activation of both IRP-1 and IRP-2. NO and H_2O_2 constitute distinct signals to IRPs, as evident from the target specificity and biochemical parameters (kinetics, okadaic acid sensitivity, and sensitivity to inducer withdrawal). This was not anticipated, as the biochemistry of NO is closely related to that of reactive oxygen intermediates (29).

The delayed responses of IRP-1 and IRP-2 to NO and to iron deficiency cannot be attributed to pharmacological properties of the compounds used, i.e., SNAP and desferrioxamine, respectively: desferrioxamine is rapidly taken up into cells, reaching a plateau within 60 min (33), while SNAP readily releases diffusible NO into aqueous solutions (11). The kinetics of IRP induction were previously also studied in the murine macrophage cell line RAW 264.7 (8). Stimulation of these cells with gamma interferon and lipopolysaccharide induces an NOS and results in a slow, NO-dependent increase in IRE-binding activity within 5 to 12 h. The kinetics of NO synthesis were monitored indirectly by measuring the appearance of nitrite in the culture medium, which precedes IRP activation by several hours (8). Thus, our direct analysis of the kinetics of IRP-1 and IRP-2 induction by NO yields data that are consistent with that study and suggests that the delayed activation of IRE-binding activity in the stimulated macrophages reflects the slow response of IRPs to NO. The results shown in Fig. 3 to 5 suggest that the activation pathways stimulated by NO and by iron deficiency may converge, on the basis of the close resemblances between their IRP activation parameters: first, their target specificities, as both IRP-1 and IRP-2 respond to these two signals; second, the fact that the patterns of kinetic activation of IRP-1 and IRP-2 by iron starvation and NO are very similar (Fig. 3); and third, that transient exposure of cells to iron chelators and NO donors is insufficient to induce the execution of activation (Fig. 5A).

How, then, does NO operate the delayed-response pathway? Previous data have suggested that NO (or peroxynitrite generated from NO) can exert a direct effect on the 4Fe-4S cluster of IRP-1, at least in vitro (5, 8, 21). Our data are consistent with these findings and in addition show that this effect is

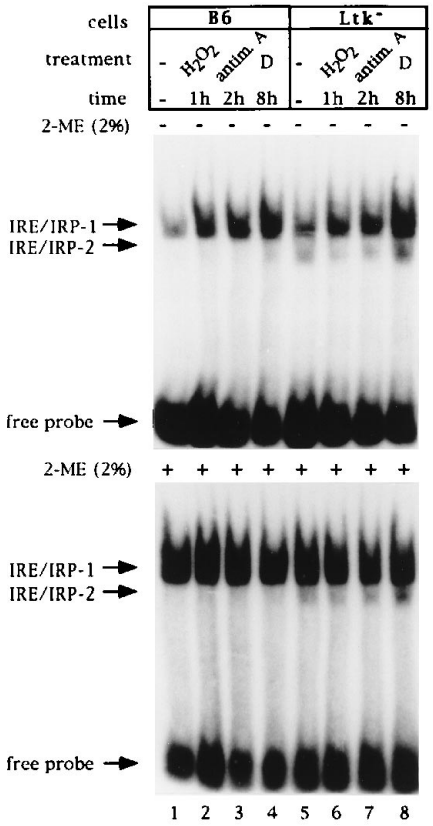

FIG. 6. Induction of IRP-1 by pharmacological modulation of respiratory chain activity. B6 (lanes 1 to 4) or Ltk$^-$ (lanes 5 to 8) cells were left untreated (lanes 1 and 5) or were treated with 100 μM H_2O_2 for 1 h (lanes 2 and 6), 100 μM antimycin (antim.) A for 2 h (lanes 3 and 7), or 100 μM desferrioxamine (D) for 8 h (lanes 4 and 8). Cytoplasmic extracts (25 μg) were analyzed by EMSA with 25,000 cpm of ^{32}P-labelled IRE probe in the absence (top panel) or presence (bottom panel) of 2% 2-ME. The positions of IRE–IRP-1 and IRE–IRP-2 complexes and of excess free IRE probe are indicated by arrows. Antimycin A (40 mM) was dissolved in ethanol; the solvent alone has no effect on IRP activity (not shown).

kinetically slow in vivo (Fig. 3). However, since the release of NO by SNAP or NOC-18 is very fast and NO is freely diffusible, one would anticipate a more rapid induction of IRP-1 by these drugs if the basis for this was a direct attack by NO on IRP-1 (perhaps the cluster). Could NO (which readily reacts with iron) affect the iron pool required for IRP-1 cluster reformation rather than destabilize the cluster? NO may sequester low-molecular-weight iron in the form of iron-nitrosyl complexes, a consideration that needs further experimental testing. Thus, the delayed-response pathway operated by NO and by iron deficiency may not affect cluster stability per se but may depend on a decrease in the size of the intracellular iron pool below a critical threshold, leading to a slow shift of the equilibrium towards the iron-free apoIRP-1. This model would also offer a common denominator to account for the differential downstream regulation of IRP-1 and IRP-2. Both proteins are controlled by a regulatory iron pool but then respond differently, by Fe-S cluster switching (IRP-1) and protein stabilization (IRP-2). Notably, iron-nitrosyl complexes have been detected by electron paramagnetic resonance spectroscopy in cytotoxic activated macrophages that release NO (32) and in L1210 leukemia cells cocultured with cytotoxic activated macrophages (9).

By contrast to the delayed-response pathways, we suggest that IRP-1 induction by H_2O_2 via the fast-response pathway may be caused by the accelerated turnover of the iron-sulfur cluster of IRP-1. The requirement for cellular integrity (36, 43), the role of phosphorylation implied by the sensitivity to okadaic acid (43), and the effects elicited upon removal of H_2O_2 (Fig. 6) suggest that a signal transduction pathway is involved in triggering IRP-1 induction, most likely by the removal of the 4Fe-4S cluster (43). H_2O_2 rapidly (5 to 15 min) induces a response program (induction phase), which can be executed even when the effector is no longer present (execution phase). It is conceivable that certain cells may lack components required to operate this oxidative stress response pathway, while most cells would be predicted to modulate IRP-1 activity by the more "passive" Fe-S cluster assembly-disassembly equilibrium mechanism. Likewise, conditions may exist under which NO rapidly activates IRP-1, possibly by affecting the levels of reactive oxygen intermediates in cells. Further definition of the fast-response pathway may lead to the identification of novel cluster-removing factors, reminiscent of the role of protein phosphatases.

The failure of H_2O_2 to induce IRP-2 is consistent with recent data suggesting that iron regulation of IRP-2 does not require an IRP-1-type iron-sulfur cluster (27). The minor level of IRP-2 activation by H_2O_2 might reflect a posttranslational response of a functionally negligible pool of IRP-2, which is small as judged by the instability of IRP-2 in cells that are not iron deficient (18, 22, 45). The relative specificity of H_2O_2 for IRP-1 predicts that cell types and tissues that predominantly express IRP-1 will respond to oxidative stress more profoundly than cells in which IRP-2 is highly expressed. It has been reported that IRP-2 is most highly expressed in the brain (23, 45), intestine (23), and heart and muscle (16). We suggest that the differential susceptibilities of IRP-1 and IRP-2 to H_2O_2 may form a basis for tissue-specific regulation of IRE-containing mRNAs.

Physiological and pathophysiological implications of IRP-1 regulation by H_2O_2. We have previously shown that IRP-1 induction by H_2O_2 augments TfR mRNA expression and suppresses ferritin biosynthesis (43). Thus, under conditions of excess of H_2O_2, the predicted increase in the intracellular iron concentration is highly toxic in light of the well-established Fenton chemistry. Moreover, a transient (15-min) exposure of cells to H_2O_2 induces complete IRP-1 activation that is sustained for several hours (Fig. 5B). These results may have implications for the understanding of the so-called hypoxia-reperfusion injury following heart attacks and strokes. Conceivably, the increased H_2O_2 concentration during the reperfusion phase (50) will induce a prolonged state of IRP-1 activation, leading to increased iron uptake and reduced iron detoxification into ferritin. Interestingly, pharmacological iron chelation in animal models (25) or high ferritin levels in cultured porcine aortic endothelial cells (1) have been found to be protective against ischemia-reperfusion injury.

The results shown in Fig. 6 demonstrate that pharmacological modulation of the respiratory chain which leads to increased generation of mitochondrial reactive oxygen intermediates affects IRP-1 activity, and they provide experimental evidence for the regulation of IRP-1 as a result of respiratory chain activity. This finding may have to be interpreted in the context of our recent observation that two Krebs cycle enzymes (mammalian mitochondrial aconitase and the iron-sulfur subunit of *Drosophila melanogaster* succinate dehydrogenase) are translationally repressed by active IRP-1 in vitro (13). Taken together, both results are consistent with the possibility that IRP-1 and reactive oxygen intermediates represent components of a novel regulatory network that allows feedback con-

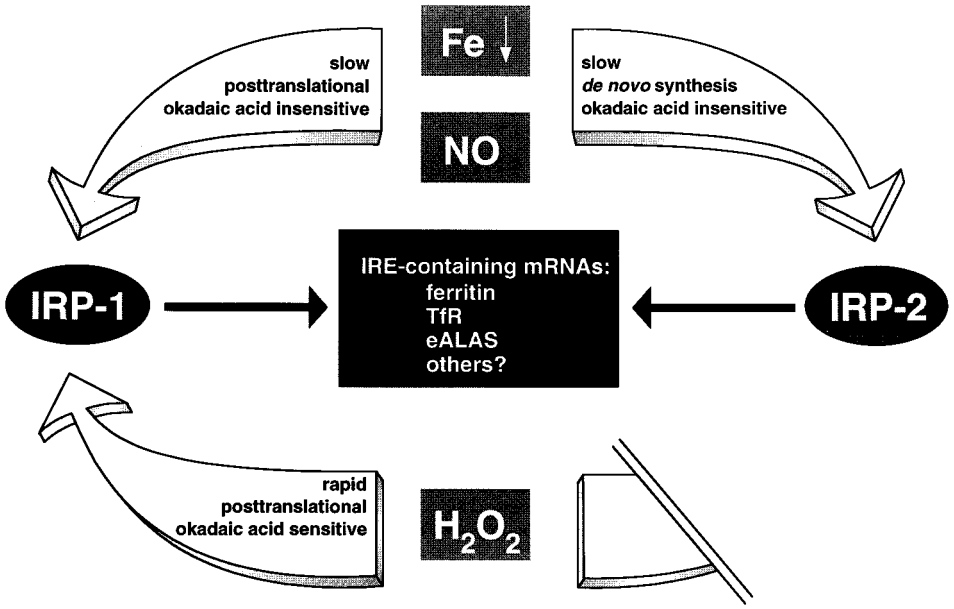

FIG. 7. Schematic representation of signalling-response relationships and characteristics for IRP-1 and IRP-2. Cells respond to iron starvation and NO by slow activation of both IRP-1 and IRP-2 by a mechanism insensitive to okadaic acid. In contrast, oxidative stress by H_2O_2 results in rapid activation of IRP-1 alone, which is (under certain conditions) okadaic acid sensitive (see text). Under all circumstances, IRP-1 activation is posttranslational, while the activation of IRP-2 requires de novo protein synthesis. Activated IRP-1 and IRP-2 both regulate the fate of IRE-containing mRNAs (including ferritin, TfR, erythroid 5-aminolevulinate synthase [eALAS], and others).

trol over mitochondrial energy metabolism. This model requires further exploration.

ACKNOWLEDGMENTS

We thank Iain Mattaj for antibodies against U1A protein, and we thank Jeremy Brock and the members of our group for comments on the manuscript.

This work was supported in part by an EU Human Capital Mobility fellowship to K.P., a Humboldt Foundation fellowship to G.W., and a grant from the Deutsche Forschungsgemeinschaft to M.W.H.

REFERENCES

1. **Balla, J., H. S. Jacob, G. Balla, K. Nath, J. W. Eaton, and G. M. Vercellotti.** 1993. Endothelial-cell heme uptake from heme proteins: induction of sensitization and desensitization to oxidative damage. Proc. Natl. Acad. Sci. USA **90:**9285–9289.
2. **Binder, R., J. A. Horowitz, J. P. Basilion, D. M. Koeller, R. D. Klausner, and J. B. Harford.** 1994. Evidence that the pathway of transferrin receptor mRNA degradation involves an endonucleolytic cleavage within the 3′ UTR and does not involve poly(A) tail shortening. EMBO J. **13:**1969–1980.
3. **Boveris, A., and B. Chance.** 1973. The mitochondrial generation of hydrogen peroxide. General properties and effect of hyperbaric oxygen. Biochem. J. **134:**707–716.
4. **Casey, J. L., M. W. Hentze, D. M. Koeller, S. W. Caughman, T. A. Rouault, R. D. Klausner, and J. B. Harford.** 1988. Iron-responsive elements: regulatory RNA sequences that control mRNA levels and translation. Science **240:**924–928.
5. **Castro, L., M. Rodriguez, and R. Radi.** 1994. Aconitase is readily inactivated by peroxynitrite, but not by its precursor, nitric oxide. J. Biol. Chem. **269:** 29409–29415.
6. **Constable, A., S. Quick, N. K. Gray, and M. W. Hentze.** 1992. Modulation of the RNA-binding activity of a regulatory protein by iron *in vitro*: switching between enzymatic and genetic function? Proc. Natl. Acad. Sci. USA **89:** 4554–4558.
7. **Dandekar, T., R. Stripecke, N. K. Gray, B. Goossen, A. Constable, H. E. Johansson, and M. W. Hentze.** 1991. Identification of a novel iron-responsive element in murine and human erythroid δ-aminolevulinic acid synthase mRNA. EMBO J. **10:**1903–1909.
8. **Drapier, J. C., H. Hirling, J. Wietzerbin, P. Kaldy, and L. C. Kühn.** 1993. Biosynthesis of nitric oxide activates iron regulatory factor in macrophages. EMBO J. **12:**3643–3649.
9. **Drapier, J. C., C. Pellat, and Y. Henry.** 1991. Generation of EPR-detectable nitrosyl-iron complexes in tumor target cells cocultured with activated macrophages. J. Biol. Chem. **266:**10162–10167.
10. **Emery-Goodman, A., H. Hirling, L. Scarpellino, B. Henderson, and L. C. Kühn.** 1993. Iron regulatory factor expressed from recombinant baculovirus: conversion between the RNA-binding apoprotein and Fe-S cluster containing aconitase. Nucleic Acids Res. **21:**1457–1461.
11. **Feelisch, M.** 1991. The biochemical pathways of nitric oxide formation from nitrovasodilators: appropriate choise of exogenous NO donors and aspects of preparation and handling of aqueous NO solutions. J. Cardiovasc. Pharmacol. **17**(Suppl. 3)**:**S25–S33.
12. **Gray, N. K., and M. W. Hentze.** 1994. Iron regulatory protein prevents binding of the 43S translation pre-initiation complex to ferritin and eALAS mRNAs. EMBO J. **13:**3882–3891.
13. **Gray, N. K., K. Pantopoulos, T. Dandekar, B. A. C. Ackrell, and M. W. Hentze.** 1996. Translational regulation of mammalian and drosophila citric acid cycle enzymes via iron-responsive elements. Proc. Natl. Acad. Sci. USA **93:**4925–4930.
14. **Gray, N. K., S. Quick, B. Goossen, A. Constable, H. Hirling, L. C. Kühn, and M. W. Hentze.** 1993. Recombinant iron regulatory factor functions as an iron-responsive element-binding protein, a translational repressor and an aconitase. A functional assay for translational repression and direct demonstration of the iron switch. Eur. J. Biochem. **218:**657–667.
15. **Green, L. C., D. A. Wagner, J. Glogowski, P. L. Skipper, J. S. Wishnok, and S. R. Tannenbaum.** 1982. Analysis of nitrate, nitrite and [^{15}N] nitrate in biological fluids. Anal. Biochem. **126:**131–138.
16. **Guo, B., F. M. Brown, J. D. Phillips, Y. Yu, and E. A. Leibold.** 1995. Characterization and expression of iron regulatory protein 2 (IRP2). Presence of multiple IRP2 transcripts regulated by intracellular iron levels. J. Biol. Chem. **270:**16529–16535.
17. **Guo, B., J. D. Phillips, Y. Yu, and E. A. Leibold.** 1995. Iron regulates the intracellular degradation of iron regulatory protein 2 by the proteasome. J. Biol. Chem. **270:**21645–21651.
18. **Guo, B., Y. Yu, and E. A. Leibold.** 1994. Iron regulates cytoplasmic levels of a novel iron-responsive element-binding protein without aconitase activity. J. Biol. Chem. **269:**24252–24260.
19. **Haile, D. J., T. A. Rouault, J. B. Harford, M. C. Kennedy, G. A. Blondin, H. Beinert, and R. D. Klausner.** 1992. Cellular regulation of the iron-responsive element binding protein: disassembly of the cubane iron-sulfur cluster results in high-affinity RNA binding. Proc. Natl. Acad. Sci. USA **89:**11735–11739.
20. **Haile, D. J., T. A. Rouault, C. K. Tang, J. Chin, J. B. Harford, and R. D. Klausner.** 1992. Reciprocal control of RNA-binding and aconitase activity in the regulation of the iron-responsive element binding protein: role of the iron-sulfur cluster. Proc. Natl. Acad. Sci. USA **89:**7536–7540.
21. **Hausladen, A., and I. Fridovich.** 1994. Superoxide and peroxynitrite inactivates aconitases, but nitric oxide does not. J. Biol. Chem. **269:**29405–29408.

22. **Henderson, B. R., and L. C. Kühn.** 1995. Differential modulation of the RNA-binding proteins IRP-1 and IRP-2 in response to iron. IRP-2 inactivation requires translation of another protein. J. Biol. Chem. **270:**20509–20515.
23. **Henderson, B. R., C. Seiser, and L. C. Kühn.** 1993. Characterization of a second RNA-binding protein in rodents with specificity for iron-responsive elements. J. Biol. Chem. **268:**27327–27334.
24. **Hentze, M. W., T. A. Rouault, J. B. Harford, and R. D. Klausner.** 1989. Oxidation-reduction and the molecular mechanism of a regulated RNA-protein interaction. Science **244:**357–359.
25. **Hershko, C.** 1994. Control of disease by selective iron depletion: a novel therapeutic strategy utilizing iron chelators. Baillieres Clin. Haematol. **7:**965–1000.
26. **Hunter, T.** 1995. Protein kinases and phosphatases: the yin and yang of protein phosphorylation and signaling. Cell **80:**225–236.
27. **Iwai, K., R. D. Klausner, and T. A. Rouault.** 1995. Requirements for iron-regulated degradation of the RNA binding protein, iron regulatory protein 2. EMBO J. **14:**5350–5357.
28. **Kennedy, M. C., L. Mende-Mueller, G. A. Blondin, and H. Beinert.** 1992. Purification and characterization of cytosolic aconitase from beef liver and its relationship to the iron-responsive element binding protein. Proc. Natl. Acad. Sci. USA **89:**11730–11734.
29. **Khan, A. U., and T. Wilson.** 1995. Reactive oxygen species as cellular messengers. Chem. Biol. **2:**437–445.
30. **Klausner, R. D., T. Rouault, and J. B. Harford.** 1993. Regulating the fate of mRNA: the control of cellular iron metabolism. Cell **72:**19–28.
31. **Kühn, L. C.** 1994. Molecular regulation of iron proteins. Baillieres Clin. Haematol. **7:**763–785.
32. **Lancaster, J. R., Jr., and J. B. Hibbs, Jr.** 1990. EPR demonstration of iron-nitrosyl complex formation by cytotoxic activated macrophages. Proc. Natl. Acad. Sci. USA **87:**1223–1227.
33. **Laub, R., Y.-J. Schneider, J.-N. Octave, A. Trouet, and R. R. Crichton.** 1985. Cellular pharmacology of deferrioxamine B and derivatives in cultured rat hepatocytes in relation to iron mobilization. Biochem. Pharmacol. **34:**1175–1183.
34. **Leibold, E. A., and H. N. Munro.** 1988. Cytoplasmic protein binds *in vitro* to a highly conserved sequence in the 5′ untranslated regions of ferritin heavy- and light-subunit mRNAs. Proc. Natl. Acad. Sci. USA **85:**2171–2175.
35. **Lipton, S. A., Y.-B. Choi, Z.-H. Pan, S. Z. Lei, H.-S. V. Chen, N. J. Sucher, J. Loscalzo, D. J. Singel, and J. S. Stamler.** 1993. A redox-based mechanism for the neuroprotective and neurodestructive effects of nitric oxide and related nitroso-compounds. Nature (London) **364:**626–632.
36. **Martins, E. A. L., R. L. Robalinho, and R. Meneghini.** 1995. Oxidative stress induces activation of a cytosolic protein responsible for control of iron uptake. Arch. Biochem. Biophys. **316:**128–134.
37. **Melefors, Ö., B. Goossen, H. E. Johansson, R. Stripecke, N. K. Gray, and M. W. Hentze.** 1993. Translational control of 5-aminolevulinate synthase mRNA by iron-responsive elements in erythroid cells. J. Biol. Chem. **268:**5974–5978.
38. **Melefors, Ö., and M. W. Hentze.** 1993. Translational regulation by mRNA/protein interactions in eukaryotic cells: ferritin and beyond. Bioessays **15:**85–90.
39. **Müllner, E. W., B. Neupert, and L. C. Kühn.** 1989. A specific mRNA binding factor regulates the iron-dependent stability of cytoplasmic transferrin receptor mRNA. Cell **58:**373–382.
40. **Oria, R., L. Sanchez, T. Houston, M. W. Hentze, F. Y. Liew, and J. H. Brock.** 1995. Effect of nitric oxide on expression of transferrin receptor and ferritin and on cellular iron metabolism in K562 human erythroleukemia cells. Blood **85:**2962–2966.
41. **Pantopoulos, K., N. Gray, and M. W. Hentze.** 1995. Differential regulation of two related RNA-binding proteins, iron regulatory protein (IRP) and IRP_B. RNA **1:**155–163.
42. **Pantopoulos, K., and M. W. Hentze.** 1995. Nitric oxide signaling to iron-regulatory protein (IRP): direct control of ferritin mRNA translation and transferrin receptor mRNA stability in transfected fibroblasts. Proc. Natl. Acad. Sci. USA **92:**1267–1271.
43. **Pantopoulos, K., and M. W. Hentze.** 1995. Rapid responses to oxidative stress mediated by iron regulatory protein. EMBO J. **14:**2917–2924.
44. **Richardson, D. R., V. Neumannova, E. Nagy, and P. Ponka.** 1995. The effect of redox-related species of nitrogen monoxide on transferrin and iron uptake and cellular proliferation of erythroleukemia (K562) cells. Blood **86:**3211–3219.
45. **Samaniego, F., J. Chin, K. Iwai, T. A. Rouault, and R. D. Klausner.** 1994. Molecular characterization of a second iron-responsive element binding protein, iron regulatory protein 2. J. Biol. Chem. **269:**30904–30910.
46. **Tang, C. K., J. Chin, J. B. Harford, R. D. Klausner, and T. A. Rouault.** 1992. Iron regulates the activity of the iron-responsive element binding protein without changing its rate of synthesis or degradation. J. Biol. Chem. **267:**24466–24470.
47. **Walden, W. E., M. M. Patino, and L. Gaffield.** 1989. Purification of a specific repressor of ferritin mRNA translation from rabbit liver. J. Biol. Chem. **264:**13765–13769.
48. **Wassarman, D. A., N. M. Solomon, H. C. Chang, F. D. Karim, M. Therrien, and G. M. Rubin.** 1996. Protein phosphatase 2A positively and negatively regulates Ras1-mediated photoreceptor development in Drosophila. Genes Dev. **10:**272–278.
49. **Weiss, G., B. Goossen, W. Doppler, D. Fuchs, K. Pantopoulos, G. Werner-Felmayer, H. Wachter, and M. W. Hentze.** 1993. Translational regulation via iron-responsive elements by the nitric oxide/NO-synthase pathway. EMBO J. **12:**3651–3657.
50. **Zweier, J. L., P. Kuppusamy, and G. A. Lutty.** 1988. Measurement of endothelial cell free radical generation: evidence for a central mechanism of free radical injury in postischemic tissues. Proc. Natl. Acad. Sci. USA **85:**4046–4050.